Effect of vibrational modes on fluidization characteristics and solid distribution of cohesive micro- and nano-silica powders

Kamphorst, Rens; Wu, Kaiqiao; van Baarlen, Matthijs; Meesters, Gabrie M.H.; van Ommen, J. Ruud

DOI
10.1016/j.ces.2024.119911

Publication date
2024

Document Version
Final published version

Published in
Chemical Engineering Science

Citation (APA)
Kamphorst, R., Wu, K., van Baarlen, M., Meesters, G. M. H., & van Ommen, J. R. (2024). Effect of vibrational modes on fluidization characteristics and solid distribution of cohesive micro- and nano-silica powders. *Chemical Engineering Science*, *291*, Article 119911. https://doi.org/10.1016/j.ces.2024.119911

Chemical Engineering Science 291 (2024) 119911

Contents lists available at ScienceDirect

Chemical Engineering Science

journal homepage: www.elsevier.com/locate/ces

Effect of vibrational modes on fluidization characteristics and solid distribution of cohesive micro- and nano-silica powders

Rens Kamphorst *, Kaiqiao Wu, Matthijs van Baarlen, Gabrie M.H. Meesters, J. Ruud van Ommen *

Department of Chemical Engineering, Delft University of Technology, Van der Maasweg 9, Delft, 2629HZ, the Netherlands

ARTICLE INFO

Keywords:
Nano-particles
Vibro-fluidized bed
Agglomeration
Assistance methods
Cohesive particles
X-ray imaging

ABSTRACT

In this study, the impact of different vibrational modes on the fluidization characteristics of cohesive micro- and nano-silica powder was examined. Fractional pressure drop, bed expansion measurements, and X-ray imaging were utilized to characterize the fluidization quality. The densities of the emulsion phase at the top and bottom of the column were quantified and compared, providing insights into the solid distribution within the fluidized bed. In the absence of vibration, neither powder could be fluidized within the considered range of superficial gas velocities. Vertical vibration was found to initiate fluidization for both powders. In contrast, elliptical vibration failed to overcome the channelling behavior when fluidizing the micro-powder. For nano-powder, combined channelling and powder compaction occurred when the bed was subjected to elliptical vibration. For the micro-powder, it was observed that bed homogeneity was independent of vertical vibration intensity but improved with increasing superficial gas velocity. For nano-powder, intensifying vertical vibration led to segregation, likely due to agglomerate densification. Furthermore, fractional pressure drop measurements proved to be a strong tool in assessing fluidization quality, providing insights that could not be attained by conventional indicators.

1. Introduction

In recent years, there has been a growing interest in cohesive micro- and nano-powders due to their diverse applications across a range of fields, including catalysis (Qu et al., 2010; Feng and Liu, 2011), electronic devices (He et al., 2020; Matsui, 2005) and food production (Dekkers et al., 2013; Wang et al., 2014). Fluidization is often the preferred method for processing powders (Van Ommen et al., 2012; Kamphorst et al., 2022). However, powders consisting of primary particles smaller than 30 μm are typically cohesive, complicating the fluidization process. The cohesive nature of these powders stems from the scaling of inter-particle forces, with respect to particle size (Kamphorst et al., 2022; Raganati et al., 2018; Seville et al., 2000). Upon decreasing the particle size, the attractive van der Waals forces start dominating (in the absence of moisture), introducing complications for fluidization. Conventional fluidization of such powders is typically characterized by channelling and excessive agglomeration, severely limiting gas-solid contact and internal mixing (Iwadate and Horio, 1998; Chen and Pei, 1984; Alavi and Caussat, 2005). If present, these phenomena dominate the often poor fluidization behavior (Kamphorst et al., 2023; Morooka et al., 1988; Zhu et al., 2005). The reduced gas-solid interactions in such systems undermine applications targeted at the high surface-to-volume ratio of (ultra-)fine particles. Additionally, a homogeneous solid distribution within the bed – indicating superior internal mixing as well as inter-phase heat and mass transfer – is beneficial for most applications and is severely lacking when utilizing conventional fluidization with such powders. To improve the fluidization quality of cohesive powders, various techniques, such as pulsed flow (AL-Ghurabi et al., 2020; Ali et al., 2016), mechanical agitation (Alavi and Caussat, 2005) and mechanical vibration (Wu et al., 2023; Mawatari et al., 2015), are described in literature. These assistance methods have been demonstrated to disrupt channelling and reduce agglomerate sizes. Out of the assistance methods found in literature, mechanical vibration has seen the most interest from researchers. Commonly listed benefits of this technique include the lack of internals and its applicability for a broad range of powders. The vast majority of studies on this method focus solely on vertical vibration, with only a few studies considering horizontal motion. Considering that a combination of horizontal and vertical motion, resulting in an elliptical trajectory, is often applied in industrial fluidized bed dryers (Satija and Zucker, 1986; Han et al., 1991; Mohseni et al., 2019), this vibration orientation begs to be explored.

* Corresponding authors.
E-mail addresses: R.Kamphorst@tudelft.nl (R. Kamphorst), J.R.vanOmmen@tudelft.nl (J.R. van Ommen).

https://doi.org/10.1016/j.ces.2024.119911
Received 25 October 2023; Received in revised form 19 January 2024; Accepted 19 February 2024
Available online 28 February 2024

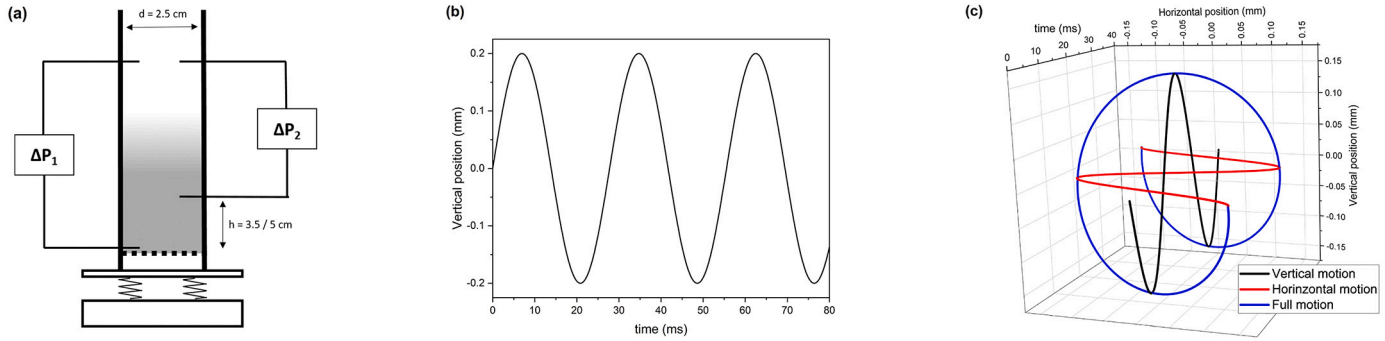

Fig. 1. (a) experimental vibro-fluidization setup with location of pressure sensors, depending on initial powder bed height, **(b)** vertical and **(c)** elliptical vibration trajectories.

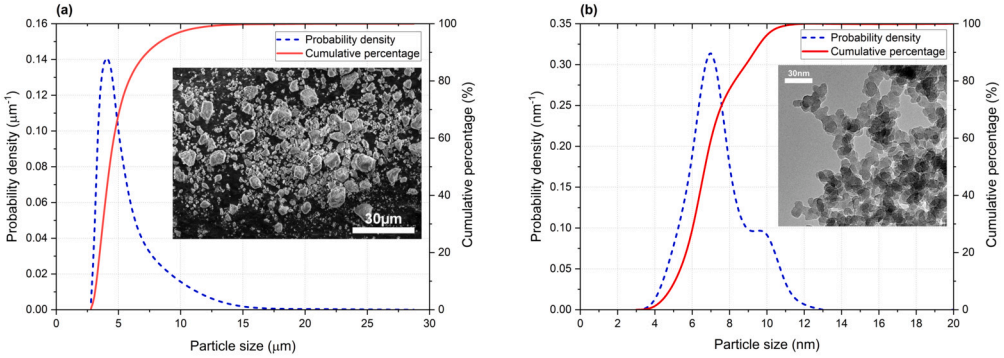

Fig. 2. Number-based particle size distributions of the used **(a)** micro- and **(b)** nano-powder.

Previous research has shown that stratification of agglomerates occurs within the fluidized bed (Wang et al., 1998), with larger agglomerates predominantly found in the bottom and smaller ones in the top of the emulsion phase. Since bed homogeneity is desirable, optimizing assistance methods necessitates insight and quantification of solid distribution. While bed homogeneity is a common focus in studies on assistance methods (Lee et al., 2019; Kaliyaperumal et al., 2011; Jaraiz et al., 1992), there is a lack of quantitative assessment in this regard.

In this study, the impact of elliptical vibration, as well as the effect of the intensity of vertical vibration, on the fluidization of cohesive micro- and nano-silica were studied. Total pressure drop and bed height expansion measurements, as well as X-ray imaging, were employed. Furthermore, we evaluated the solid distribution within vibro-fluidized beds, subjected to various vibration modes. This analysis was performed by examining the density distribution alongside the bed height, calculated from fractional pressure drop measurements.

2. Materials and methods

2.1. Experimental

For all fluidization experiments, a glass column with an inner diameter of 2.5 cm was used. Similar column sizes are commonly found in literature, both for studying the fundamentals (Zeng et al., 2008; Yang et al., 2009) and applications of fluidized beds (Li et al., 2010; Shen and Gu, 2009; Kamphorst et al., 2024). The column was filled with powder reaching a bed height of either 5.0 cm (with a ratio of initial bed height to column inner diameter $H_0/D = 2.0$), denoted as 'low', or 7.5 cm ($H_0/D = 3.0$), denoted as a 'high' initial bed height. Prior to each experiment, the powder sample was weighed on an ABJ 320-4NM scale, allowing to calculate the static pressure exhibited by a given sample in the absence of a gas flow. Dry nitrogen was supplied through a SIKA-R 3 AX distributor plate. Two pressure sensors utilized during each experiment, one of which measured the pressure drop, ΔP, from the bottom to the top of the column, the other measuring from $2/3^{rd}$ of the initial bed height to the top, as depicted in Fig. 1**a**. FSM DPS pressure sensors were used for the micro-sized particles, whereas Siemens QBM2030-1U pressure sensors were employed for the nano-powder. The setup was mounted on a PTL-40/40 vibrating table. When operating in the vertical orientation, two distinct modes were used, which will be referred to as a 'low' setting and a 'high' setting throughout this work. The 'low' intensity corresponds to the lowest setting at which the micro-powder could consistently be fluidized within the range of superficial gas velocities considered in this study. The same vibrating table was used to create both vertical and horizontal vibrations simultaneously, resulting in an elliptical motion. The relevant parameters of the selected vibrational modes are provided in Table 1.

Table 1
Amplitudes and frequencies of studied vibrational modes.

	Vibrational settings			
Label	A_x (mm)	f_x (Hz)	A_y (mm)	f_y (Hz)
Low vertical	0	0	0.20	36
High vertical	0	0	0.30	51
Elliptical	0.15	36	0.14	36

Both powders used in the experimental investigation are SiO_2 based. The micro-sized powder, Köstropur 050818, has a number-based primary particle size of 4.4 μm (d_{50}), as measured by laser diffraction (see Fig. 2**a**). The nano-sized powder, Aerosil 300, is characterized by a number-based primary particle size of 6.7 nm (d_{50}), as obtained from analysis of TEM images (see Fig. 2**b**). The dominant difference in fluidization behavior observed within cohesive powders originates from the different agglomerate structures formed by micro- and nano-powders, being single-stage or multi-stage agglomerates respectively (Kamphorst et al., 2022). Therefore, the powders considered in this study offer insights that are broadly applicable to cohesive powders as a whole.

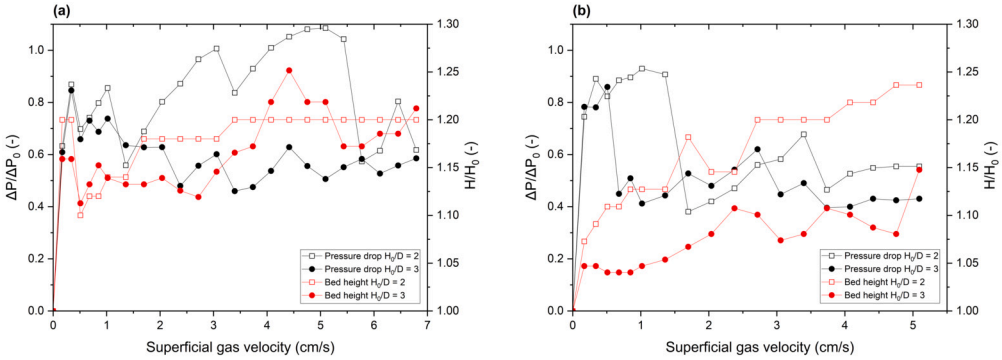

Fig. 3. Normalized pressure drop and bed expansion data from unassisted fluidization of **(a)** micro and **(b)** nano-powder.

Previous studies have shown that powder history, particularly slow compaction during storage, significantly affects the fluidization behavior of cohesive powders (Bailey, 1984; Valverde and Castellanos, 2006). To ensure reproducibility of our work, fresh powder was used for each experiment. Additionally, the powder was sieved (mesh size of 600 μm for micro- and 224 μm for nano-powder) prior to any measurement. This procedure maintained a consistent state of aeration for the powder bed prior to conducting experiments. Note that the used pore sizes are orders of magnitude larger than the primary particle size of the respective powders, therefore having a negligible impact on the particle size distributions. Moreover, since prior studies have shown fluidization behavior to change over time (Nam et al., 2004; Mogre et al., 2017), each measurement was taken 10 min after the initiation of gas flow. Unless stated otherwise, the presented data points represent the average of three separate experiments.

2.2. Density calculations

The theoretical maximum pressure drop over a fluidized bed can be calculated as per Eq. (1). Here, ΔP_0 represents the maximum theoretical pressure drop, m_{bed} the mass of powder in the column, g the gravitational acceleration, and S_{column} the cross-sectional area of the column. The fraction of fluidized material, X_f, is calculated as per Eq. (2), where P_{tot} represents the measured pressure drop over the entire bed. For the fractional measurements, the bed was divided into a bottom and top section. The bottom phase runs from the distributor plate to the location of the pressure sensor at 3.5 cm for low and 5 cm for high bed initial height, as shown in Fig. 1a. The top phase spans from the bottom sensor location to the top of the emulsion phase. The pressure drop in the top section was measured directly, while the ΔP of the bottom section was obtained by the difference between the entire bed and the top section. For calculation of the emulsion density in the top of the bed, Eq. (3) was used. Here, ΔP_{top} represents the pressure drop measured over the top section of the bed and H_{top} the height of the bed in the top section, which is equal to the total bed height, H_{bed}, minus the height of the bottom pressure sensor, H_{bot}. Note that Eq. (3) implicitly assumes the powder present above the top pressure sensor to be fully fluidized. If this condition is not fulfilled, the equation can still be used to calculate a surrogate top density. While the calculated value may not provide an adequate assessment of the fluidized state in the top section by itself in such case, the ratio between top and bottom bed densities, will still provide valuable insights into the quality of fluidization as will be shown in the result section.

$$\Delta P_0 = \frac{m_{\text{bed}} \cdot g}{S_{\text{column}}} \tag{1}$$

$$X_f = \frac{\Delta P_{\text{tot}}}{\Delta P_0} \tag{2}$$

$$\rho_{\text{top}} = \frac{\Delta P_{\text{top}}}{H_{\text{top}} \cdot g} \tag{3}$$

Additional considerations are required to calculate the density of the emulsion phase in the bottom section of the bed. The fluidized fraction is typically less than unity, meaning a fraction of the powder unagitated, not contributing to the pressure drop. This stagnant powder occupies space in the bottom section, which needs to be corrected for. Eq. (4) was used to calculate ρ_{bot}, the density in the bottom section of the bed. In this equation, ΔP_{bot} represents the pressure drop over the bottom section of the bed and ρ_b the bulk density of the powder. The ρ_{b} after sieving is 134 kg m^{-3} for micro-silica and 50 kg m^{-3} for nano-silica. For the density ratios presented in this work, the calculated bottom density was divided by the (surrogate) top density.

$$\rho_{\text{bot}} = \frac{S_{\text{column}} \cdot \Delta P_{\text{bot}}}{g \cdot \left(S_{\text{column}} \cdot H_{\text{bot}} - \frac{m_{\text{bed}}(1-X_f)}{\rho_b} \right)} \tag{4}$$

2.3. X-ray imaging

To provide additional insight in the gas-solid distribution within the fluidized bed and verify the results obtained by the fractional pressure drop measurements, X-ray imaging was performed. Experiments were performed using an in-house fast X-ray imaging set-up, utilizing a single standard industrial type X-ray tube source (Yxlon International GmbH) with a maximum energy of 150 keV working in cone beam mode and a Teledyne Dalsa Xineos 2D detector. A detailed description of this setup can be found in our previous work (Kamphorst et al., 2023).

3. Results and discussion

3.1. Unassisted fluidization

Previous research findings indicated that cohesive powders, with particle sizes comparable to those used in our study, may exhibit fluidization without the need for assistance methods (Pacek and Nienow, 1990; Yao et al., 2002). However, as can be seen in Fig. 3, unassisted operation did not yield desirable fluidization quality for the powders considered in this study. The bed expansion was observed to be relatively modest in all experiments. This expansion primarily resulted from the formation of gas channels, looser packing, and sporadic particle spouting. The significant initial pressure drop ratio, observed for all experiments, was attributed to plugs which did not break at low gas velocities, consistent with our earlier work (Kamphorst et al., 2023). At higher gas velocities, the $\Delta P/\Delta P_0$ exhibited high fluctuations due to the formation and subsequent collapse of channels coupled with occasional spouting in the upper section of the bed. Given the inherent unpredictability of the channelling behavior in unassisted fluidization of cohesive powder, attaining reproducible data becomes challenging. Therefore, the data points presented in Fig. 3 are of single experiments. Nevertheless, repeated runs yielded similarly fluctuating profiles.

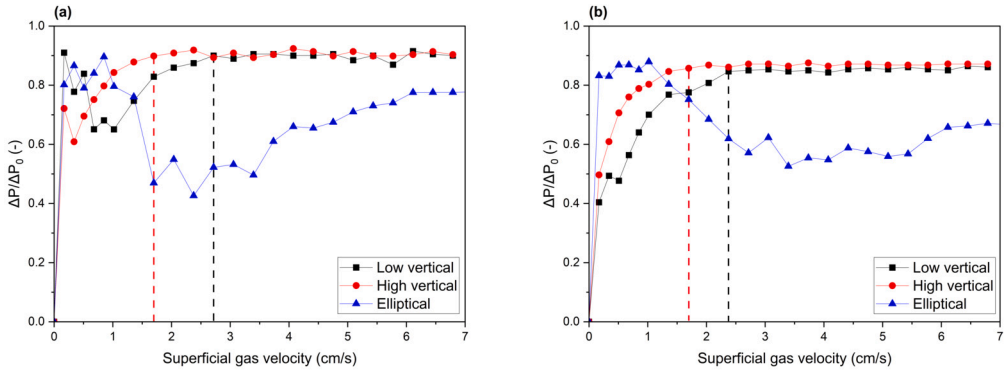

Fig. 4. Normalized pressure drop of vibro-fluidized beds consisting of micro-powder with **(a)** low and **(b)** high initial bed heights, the dashed lines indicate the minimum fluidization velocities.

3.2. Vibro-fluidization of micro-powder

The normalized pressure drop values of micro-powder beds under different vibrational modes are depicted in Fig. 4. The dashed vertical lines indicate minimum fluidization velocities, corresponding to the first pressure drop value that falls within a 1% range of the average of the five consecutive data points. At low-intensity vertical and elliptical vibration, the values appear to be irregular at low gas velocities, irrespective of initial bed height. This behavior corresponds to slugging as well as the formation and subsequent collapse of gas channels, comparable to unassisted fluidization. For vertical vibration, the final $\Delta P/\Delta P_0$ all range from 0.88 to 0.91, indicating no significant dependency on vibrational intensity or initial bed height. In our prior research, utilizing the same micro-powder in a 9 cm column, vibrated at $f = 50$ Hz and $A = 1$ mm, $\Delta P/\Delta P_0$ values of up to 0.93 were found (Kamphorst et al., 2023). The similar final normalized pressure drop values, while utilizing vastly different column sizes, suggest that wall effects played not significant role during these experiments. Furthermore, the $\Delta P/\Delta P_0$ is comparable to those reported by other studies on cohesive micro powders in vibro-fluidized beds, ranging from 0.7 to 1.0 (Mawatari et al., 2003; Lee et al., 2019; Barletta and Poletto, 2012; Kaliyaperumal et al., 2011; Jiang and Fatah, 2022). A decrease in minimum fluidization velocity with respect to initial bed height can be observed, which was also found during the experiments with nano-particles. This can be explained by considering the channel dimensions. To provide a consistent gas bypass, a channel needs to span the entire bed height. A taller bed will produce longer, and comparatively more slender, channels, which are more easily disrupted, leading to improved fluidization (i.e., a lower minimum fluidization velocity). Consistent with earlier studies, an increase in vertical vibrational intensity was found to decrease the minimum fluidization velocity (Lee et al., 2019; Mawatari et al., 2015). In the case of elliptical vibration, the $\Delta P/\Delta P_0$ values remain consistently low, compared to vertical vibration. Some degree of stable fluidization is achieved, as indicated by the smooth pressure drop curve at high superficial gas velocities, compared to the one found for unassisted fluidization. However, the presence of gas channels is visually observed throughout all experiments.

Contrary to the expectation of enhancing fluidization through the introduction of additional energy, the horizontal component of elliptical vibration was found to counteract the disruptive effects of vertical vibrations. This is apparent from the comparatively low $\Delta P/\Delta P_0$ data obtained while introducing elliptical vibrations, as shown in Fig. 4. The same can be seen by considering the coefficients of variation of the obtained data, which can be found in the supplementary materials. Furthermore, looking at Fig. 4, lowering the vibrational intensity shifts the obtained results, delaying the pressure plateau at which fluidization occurs, while the trend itself is preserved, the same was demonstrated by earlier studies (Lee et al., 2019; Zhou et al., 2018; Marring et al., 1994). When considering the results of elliptical vibration however, it

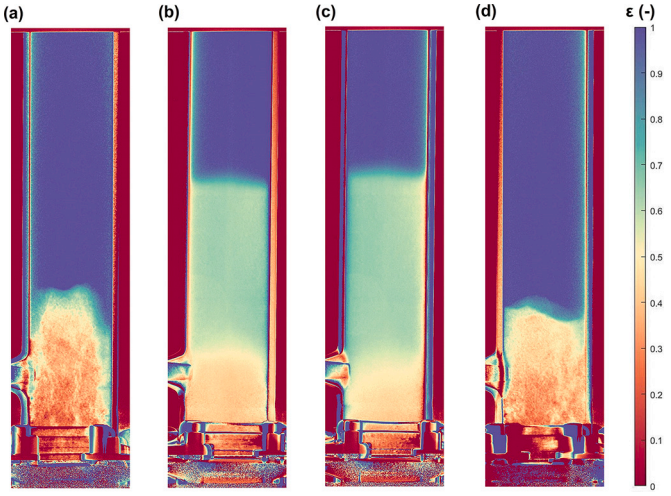

Fig. 5. 10 second average X-ray images of the bed of micro particles in a fluidized bed column with a superficial gas velocity of 3.0 cm s^{-1}, subjected **(a)** no vibration, **(b)** low intensity vertical vibration, **(c)** high intensity vertical vibration and **(d)** elliptical vibration, the legend on the right provides the gas fraction corresponding to each color.

can be seen that no such trend is visible at all, suggesting the underlying phenomena dominating this system are fundamentally different. Note that full fluidization can sometimes be obtained when applying vertical vibration of a lower intensity than used in this study. Therefore, the absence of full fluidization in all experiments conducted with elliptical vibration cannot be explained by the lower amplitude in the vertical direction considered in isolation.

It was hypothesized that this phenomenon may be attributed to the compaction of powder against the column wall induced by the horizontal motion, similar to the effect of vertical vibration in creating a dense layer near the distributor plate (Wu et al., 2023). In order to investigate this hypothesis, additional experiments were performed, using the X-ray imaging technique, to inspect the flow patterns. The results of these experiments are depicted in Fig. 5. The displayed images represent an average of 650 frames (10 s) captured 10 min after the initiation of gas flow. First of all, Fig. 5a shows channelling in the absence of any vibration applied to the system. Furthermore, since structures can be seen, even while the images are time-averaged, it can be concluded that these structures are mostly stable. In Fig. 5b and c the gas fractions of fluidized beds subjected to low and high intensity vertical vibration are displayed. These beds demonstrate significant bed expansion and a fairly homogeneous emulsion phase, indicating the absence of permanent structures. However, the bottom region of the bed is significantly denser than the top section for either vibration intensity. This phenomenon was also observed in a study by Wu et al. utilizing a sig-

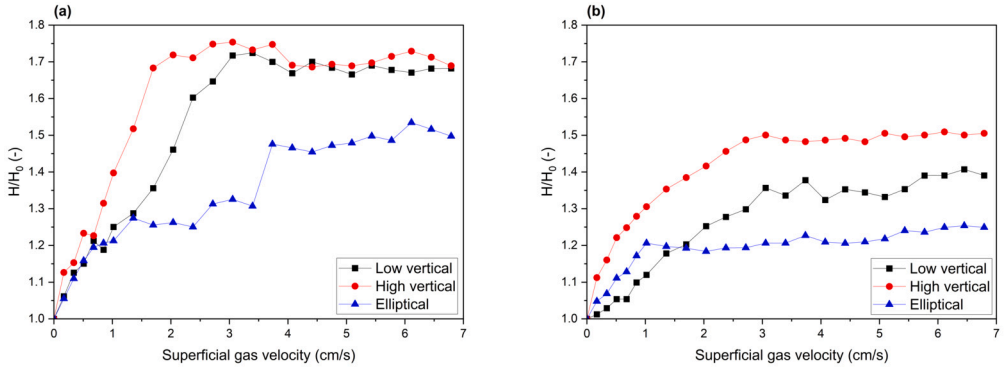

Fig. 6. Normalized bed expansions of vibro-fluidized beds consisting of micro-powder with **(a)** low and **(b)** high initial bed heights.

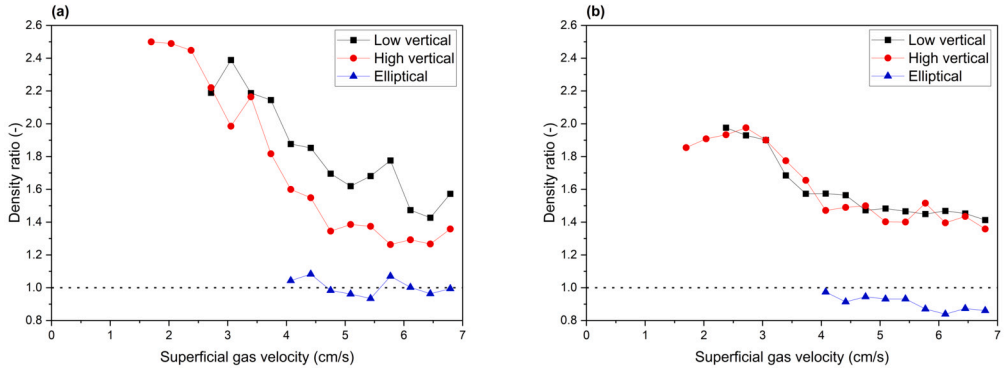

Fig. 7. Density ratios between top and bottom sections of vibro-fluidized beds consisting of micro-powder with **(a)** low and **(b)** high initial bed heights.

nificantly higher amplitude for the vibration (Wu et al., 2023). The consistent appearance of this region at the lowest intensity at which consistent fluidization can be achieved, as well as at significantly higher frequencies and amplitudes of vibration, indicates its presence to be unavoidable. The lack of long-term structures in the bottom sections does however indicate that this region is still fluidized under influence of either vertical vibration intensity. Finally Fig. 5d provided insight in the bed operated at elliptical vibration. Long-term structures can be observed with only a small fraction of the powder being fluidized. Based on the similarity observed in the flow patterns between elliptically vibrated and non-vibrated beds, it can be concluded that elliptical vibration does not have a discernible influence on the channel formation or disruption. Furthermore, these findings highlight the mitigation of vertical vibrations, when horizontal motion is employed, in a manner resulting in an elliptical motion of the system. However, these experiments do not provide conclusive evidence to determine whether this phenomenon is solely due to horizontal vibrations or the specific combination of horizontal and vertical vibrations employed in our experiments. The persistent channelling also explains the relatively low and stable normalized pressure drop values observed in Fig. 4. Additionally, the anticipated compaction of particles near the column walls was not obvious, and an accurate assessment of compaction at the bottom cannot be fully realized, as the presence of a clamp obstructed part of the view of the lower section.

The bed expansion of the micro-powder reached a plateau across all experimental conditions, as shown in Fig. 6. The comparison of the $\Delta P/\Delta P_0$ and H/H_0 graphs also reveals that the plateau in bed expansion typically occurs at higher gas velocities. This observation suggests that the expansion of the bed between the minimum fluidization velocity and the velocity at maximum bed expansion is primarily influenced by the increased dilation of the emulsion phase, rather than the additional fraction of powder becoming fluidized. Moreover, a comparison between Fig. 6a and Fig. 6b illustrates that lower initial bed heights result in higher bed expansion ratios across all vibration modes investigated. This finding indicates a potential correlation between the attenuation of vibrations throughout the powder bed, resulting in the vibrations having a greater impact on shallower powder beds. However, this limitation may be partially overcome by increasing the vibrational intensity, thereby increasing the penetration depth of the effective vibration into the bed, as suggested in Fig. 6b.

The density ratios between the bottom and top sections of the micro-powder bed, as defined in Section 2.2, are displayed in Fig. 7. The data related to vertical vibration modes spans from the minimum fluidization point to the maximum gas velocity at which experiments were performed. Across these cases, it can be observed that the density in the bottom region of the bed is approximately twice that of the top section. Previous research has indicated the occurrence of agglomerate stratification in fluidized beds containing micro- and nano-particles (Wang et al., 1998). Provided that larger agglomerates are more often found in the bottom of the bed, it is expected that the density of the emulsion phase is higher in this region since smaller agglomerates, experiencing the same gas velocity are more likely to be lifted by the gas flow, due to their lower terminal velocity. This results in a higher inter-agglomerate voidage and therefore a less dense phase. However, as mentioned earlier, the vibration itself induces the formation of a dense phase in the bottom region of a vibro-fluidized bed. Rather than segregation based on agglomerate size, the bottom phase getting hit repeatedly by the distributor plate appears to be the dominant factor leading to this dense phase. An increase in the gas velocity was found to mitigate this issue, independent of vibration intensity. It is important to note that this information cannot be deduced from the total pressure drop or bed expansion measurements. Solely relying on these indicators, one would find no further improvements in fluidization quality after 3.0 cm s^{-1}, as both $\Delta P/\Delta P_0$ and H/H_0 reach a plateau at this point, which underscores the benefits of fractional pressure drop measurements. For the elliptically vibrated beds, exhibiting no significant degree of fluidization at any of the experimental conditions, density ratios were plotted from 4 cm s^{-1} onward. The results for both initial bed heights may suggest a completely homogeneous mixture. However, effective fluidization did not occur as indicated by the pressure drop and by X-ray imaging. In-

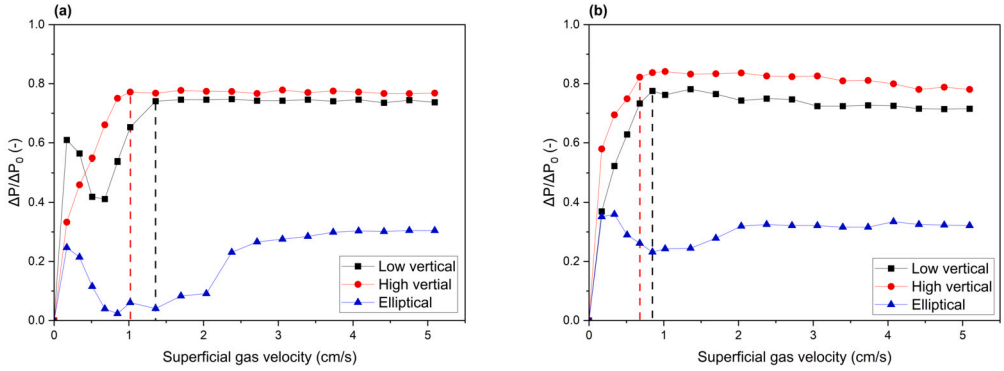

Fig. 8. Normalized pressure drop of vibro-fluidized beds consisting of nano-powder with **(a)** low and **(b)** high initial bed heights, the dashed lines indicate the minimum fluidization velocities.

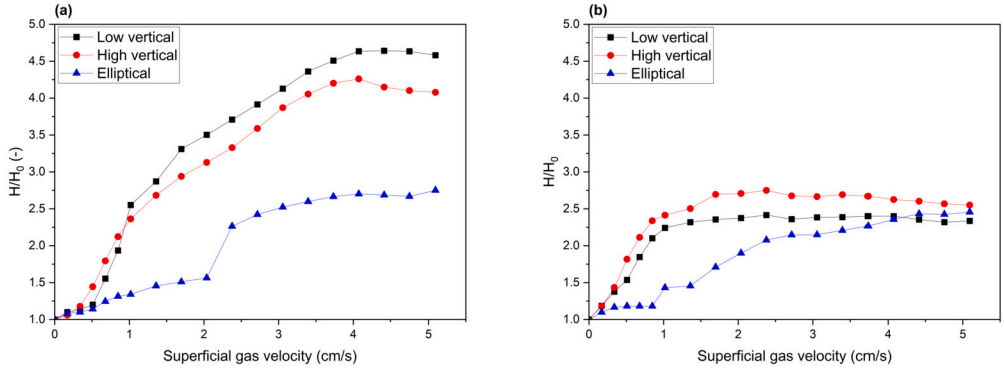

Fig. 9. Normalized bed expansions of vibro-fluidized beds consisting of nano-powder with **(a)** low and **(b)** high initial bed heights.

stead, these results indicate persistent channelling in the bottom section of the bed, resulting in a low pressure drop within that region, while occasional spouting behavior in the top of the bed causes a relatively high pressure drop in that section, resulting in a ratio less than 1. Moreover, higher initial bed heights lead to even lower density ratios due to the instability of taller and slender channels, which are more prone to collapse in the top of the bed, leading to enhanced spouting and local pressure drop values in this region. These findings reinforce the conclusion that elliptical vibration does not consistently eliminate channelling. Additionally, these results demonstrate the capability of fractional pressure drop measurements to indicate the presence of channels within the powder bed by obtaining density ratio approaching or below unity.

3.3. Vibro-fluidization of nano-powder

The pressure drop values observed during experiments conducted with nano-powder are displayed in Fig. 8. Similar to the micro-powder results, the fluctuations in some of the data at low gas velocities can be attributed to slugging and channelling phenomena. Moreover, all vibration modes exhibit a plateau in the pressure drop ratio, the elliptically vibrated bed at significantly lower values than both vertically vibrated ones. High intensity vertical vibrations consistently exhibit the lowest minimum fluidization velocity, followed by low intensity vertical vibrations, due to its low normalized pressure drop value, the elliptically vibrated bed is not considered to be adequately fluidized. A discussion on the coefficients of variation corresponding to the pressure drop data can be found in the supplementary materials. As for the micro-powder, an increased aspect ratio of the bed lowers the minimum fluidization velocity due to the presence of less stable channels.

According to Fig. 8 and Fig. 9, high pressure drop values are accompanied by high bed expansion ratios. As for the micro-powder, the peak values of H/H_0 are attained at gas velocities beyond u_{mf} and higher initial bed heights result in lower bed expansion ratios, indicating signal attenuation throughout the beds. Additionally, while the pressure drop values were low, substantial bed expansion is observed with elliptical vibration. Zhang et al. reported similar bed expansions for a horizontally vibrated bed of Aerosil 300 at 33.4 Hz (Zhang and Zhao, 2010), which aligns with our findings for elliptical vibration. In that study, the conclusion that the Aerosil 300 was well-fluidized was solely based on bed expansion as no pressure drop values were reported. Our pressure drop results do however indicate that only a limited amount of powder is agitated, highlighting the limitations of bed expansion data in reliably assessing the fluidization quality of cohesive powders. The normalized pressure drop plateau values for vertical vibration found in this work range from 0.75 to 0.85. This is reasonably close to the range of 0.82–1.1 found in other studies on vibro-fluidization of nanopowders (Kaliyaperumal et al., 2011; Nam et al., 2004; An and Andino, 2019).

While the low pressure drop values observed with elliptical vibration can be partially explained by ineffective channel disruption, as discussed in Section 3.2, the existence of a plateau in normalized pressure drop, accompanied by a significant bed expansion, suggests at least part of the bed is fluidized. It is therefore anticipated that channel destabilization is not the sole contributing factor. To elucidate, additional experiments were conducted. Similar to how vertical vibration induces compaction of the bottom fraction of the bed, we hypothesized that the column walls would provide an additional source of compaction due to the horizontal component of the elliptical motion. The low bulk density of the silica nano-powder complicates the exact determination of density differences with X-ray imaging, necessitating the use of alternative methods. To this end, nano-powder was fluidized at 3 $cm\,s^{-1}$ for 10 min with an initial H/D of 2.0 for each vibration mode. After terminating the gas flow, loose powder was carefully extracted using a suction probe, inserted from the top of the column. Subsequently, the windbox was then removed, and all remaining powder, compacted on the column wall and distributor plate, was collected. The weight fraction of the collected powders were presented in Fig. 10, each data

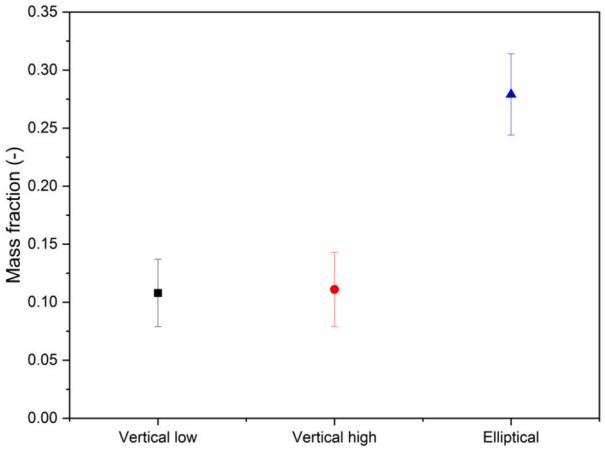

Fig. 10. Fraction of compacted nano-powder present in the system after fluidizing under different vibration conditions, averages of 5 measurements, error bars correspond to the standard deviation.

point representing an average of five measurements. The results indicate no significant difference between low and high intensity vertical vibrations. The nano-powder being predominantly found at the bottom of the column after employing either vertical vibration mode, supports the idea that this compaction results from tapping by the distributor plate. In contrast, when elliptical vibration was employed, the amount of compacted powder nearly triples compared to that observed in vertical vibrations. Although not quantified, visual observations confirm a substantial amount of powder adhering to the column walls. It should be noted that triboelectric forces, causing the nano-powder to adhere to the column walls, may contribute to this phenomenon as well. The observed compaction can account for the relatively low pressure drop observed during the fluidization of the nano-powder with elliptical vibration, as depicted in Fig. 8, as this fraction of powder does not actively participate in the fluidization process.

In Fig. 11, the influence of gas velocity on the density ratios of nano-powder under the selected vibration modes is presented. As with the micro-powder analysis, the ratios are plotted from u_{mf} onwards for vertical vibrations, while for elliptical vibration, the gas velocities corresponding to the pressure drop plateaus are displayed. The density ratios under both vertical intensities are 1.5 to 2 times higher than those for the micro-powder. This observation can be attributed to the relatively denser bottom section of the nano-powder, stemming from its higher compactability. Furthermore, higher intensities were found to depress the bed homogeneity. However, based on the findings presented in Fig. 10, this is not attributable to variations in compacted regions with increased vibration intensity. Rather, we hypothesize that agglomerates densify, leading to enhanced stratification within the emulsion phase. Existing literature indicates that nano-particle agglomerates undergo densification over time, the higher vibration intensity is expected to increase agglomerate-agglomerate and agglomerate-wall collisions, amplifying this densification. The densification process is associated with a decrease in agglomerate size (Mogre et al., 2017), which, combined with other studies demonstrating reduced agglomerate size with increased vibration intensities (Kaliyaperumal et al., 2011; Barletta and Poletto, 2012), substantiates this hypothesis. In the case of elliptical vibration, the density ratios are significantly higher (note the axis break in Fig. 11b), indicating poor internal mixing within the emulsion phase. It is important to note that the observed poor solid distribution cannot be attributed to the compacted fractions shown in Fig. 10, as they were measured to exhibit a minimal pressure drop. Instead, it is suspected that the increased particle-wall collisions resulting from the horizontal component of the elliptical motion results in denser agglomerates, amplifying the density gradient along the bed height. Additionally, the considerable portion of un-fluidized powder introduces sensitivity to the calculated density ratios, as these results rely on the correction method for the volume of the bottom section, as seen in Eq. (4). It is suspected that the density of the un-fluidized fraction may deviate from the bulk density, possibly reflecting a tapped density. It is worth noting that such a deviation may lead to the results presenting an exaggerated representation of the actual density ratio.

3.4. Comparative analysis of micro- and nano-silica vibro-fluidization

Upon examining the datasets obtained from all experiments collectively, several overarching conclusions can be drawn. Neither powder could be fluidized without the aid of an assistance method, while high and low intensity vertical vibrations were effective in achieving a fluidized state for both powders. Comparing beds with high and low initial bed heights, the latter consistently demonstrated higher bed expansion ratios, suggesting attenuation of the vibration signal through the bed. Furthermore, higher initial bed heights consistently corresponded with lower minimum fluidization velocities, attributed to less channel integrity in taller bed. However, notable differences are found when considering the density ratios of the respective powders. With increasing vibration intensity, the fluidized nano-powder exhibited reduced homogeneity, whereas no significant effect was observed for micro-powder. This discrepancy can be explained by the distinctive agglomeration processes inherent to micro- and nano-powders. Micro-powders undergo agglomeration through the clustering of primary particles, driven by attractive inter-particle forces, often referred to as ‘single-stage agglomeration’ (Kamphorst et al., 2022). In contrast, nano-particles form multi-staged agglomerates, wherein primary particles are sintered into aggregates during the production process. These aggregates can then cluster together to form simple agglomerates, which further stick together to create complex agglomerates (Kamphorst et al., 2022; Yao et al., 2002). Importantly, each stage of this multi-stage agglomeration incorporates additional voids into the structure, resulting in a lower density and increased compactability.

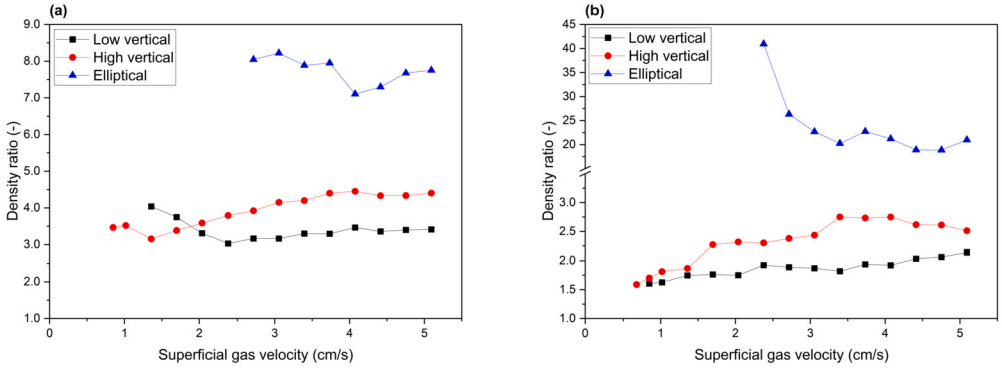

Fig. 11. Density ratios between top and bottom sections of vibro-fluidized beds consisting of nano-powder with **(a)** low and **(b)** high initial bed heights.

The difference in behavior of the two powders when subjected to increased vibration intensity is therefore attributed to the disparities in agglomerate structure and characteristics, particularly the compactability of the formed agglomerates. It is worth noting that the exact particle size at which single-stage transitions into multi-stage agglomeration is not well-defined (Kamphorst et al., 2022), limiting the predictability of fluidization behavior.

4. Conclusion

In this study, we investigated the impact of vibrational orientation and intensity on the bed homogeneity of fluidized micro- and nano-silica. Bed expansion and fractional pressure drop values were collected to quantify fluidization quality. In the absence of mechanical vibration, both powders exhibited slugging and channelling, resulting in poor fluidization. However, vertical vibration enabled fluidization of both micro- and nano-powders, as evidenced by increased pressure drop ratios and significant bed expansions. The solid distribution of micro-powder is enhanced by increasing the superficial gas velocity. In contrast, bed homogeneity was unaffected by superficial gas velocity when considering nano-particles. Furthermore, increasing the vertical vibration intensity in such systems led to large density differences within the bed, attributed agglomerate compaction. Elliptical vibration, already applied in industry for non-cohesive powder fluidization, did not yield a desirable fluidization quality for either powder. For micro-particles, this mode was incapable of adequately disrupting channels, whereas for nano-particles, this orientation additionally led to a significant increase in powder compaction. Furthermore, vertical vibration introduces an unavoidable high-density region in the bottom of the bed, restricting the effectiveness of this assistance method. Combined with indicated signal attenuation over the system, it is implied that mechanical vibration, of any orientation, has limited benefits for the fluidization of cohesive powders at large scale. Therefore, research into other assistance methods, that may avoid these specific issues, is encouraged. Additionally, while the elliptical orientation was found to be inefficient, fundamental understanding of its ineffectiveness is incomplete. Combinations of horizontal and vertical motion resulting in other trajectories, may still provide benefits; further research into these methods is required to allow for generalization of the results regarding the field vibro-fluidization of cohesive powders as a whole. Specifically, a study on sole horizontal vibration, utilizing fractional pressure drops to assess the solid distribution throughout the column would provide valuable insights, especially considering the few available studies on this topic and their limited assessment of fluidization quality.

Finally, our findings emphasize the limitations of relying on total pressure drop and bed extension as indicators of fluidization quality. Fractional pressure drop measurements are recommended for studying fluidized beds and optimizing assistance methods as they provide insight into solid distribution, while being easy to implement. Additionally, fractional pressure drop measurements were found to be a useful tool to indicate the presence of channels within the system.

List of symbols

ρ	Density	[kg m^{-3}]
A	Amplitude	[mm]
f	Frequency	[Hz]
g	Gravitational acceleration	[m s^{-2}]
H	Measured bed height	[m]
H_0	Bed height prior to gas flow initiation	[m]
m_{bed}	Mass of powder in the bed	[kg]
ΔP	Measured pressure drop	[Pa]
ΔP_0	Theoretical pressure drop	[Pa]
S_{column}	Cross-sectional area of column	[m^2]
X_f	Fraction of fluidized material	[–]

CRediT authorship contribution statement

Rens Kamphorst: Conceptualization, Formal analysis, Investigation, Methodology, Validation, Visualization, Writing – original draft. **Kaiqiao Wu:** Formal analysis, Validation, Writing – original draft. **Matthijs van Baarlen:** Formal analysis, Methodology, Validation. **Gabrie M.H. Meesters:** Funding acquisition, Supervision, Writing – review & editing. **J. Ruud van Ommen:** Funding acquisition, Supervision, Writing – review & editing.

Declaration of competing interest

The authors declare that they have no known competing financial interests or personal relationships that could have appeared to influence the work reported in this paper.

Acknowledgements

This work is part of the Advanced Research Center for Chemical Building Blocks, ARC-CBBC, which is co-founded and co-financed by the Dutch Research Council (NWO) and the Netherlands Ministry of Economic Affairs and Climate Policy. Grant number: 2020.023.A.TUD.1.

Appendix A. Supplementary material

Supplementary material related to this article can be found online at https://doi.org/10.1016/j.ces.2024.119911.

References

Al-Ghurabi, E., Shahabuddin, M., Siva Kumar, N., Asif, M., 2020. Deagglomeration of ultrafine hydrophilic nanopowder using low-frequency pulsed fluidization. Nanomaterials 10, 388. https://doi.org/10.3390/nano10020388.

Alavi, S., Caussat, B., 2005. Experimental study on fluidization of micronic powders. Powder Technol. 157 (1), 114–120. https://doi.org/10.1016/j.powtec.2005.05.017. 4th French Meeting on Powder Science and Technology.

Ali, S., Al-Ghurabi, E., Ajbar, A., Mohammed, Y., Boumaza, M., Asif, M., 2016. Effect of frequency on pulsed fluidized beds of ultrafine powders. J. Nanomater. 2016, 1–12. https://doi.org/10.1155/2016/4592501.

An, K., Andino, J.M., 2019. Enhanced fluidization of nanosized TiO_2 by a microjet and vibration assisted (MVA) method. Powder Technol. 356, 200–207. https://doi.org/10.1016/j.powtec.2019.08.011.

Bailey, A., 1984. Electrostatic phenomena during powder handling. Powder Technol. 37, 71–85. https://doi.org/10.1016/0032-5910(84)80007-8.

Barletta, D., Poletto, M., 2012. Aggregation phenomena in fluidization of cohesive powders assisted by mechanical vibrations. Powder Technol. 225, 93–100. https://doi.org/10.1016/j.powtec.2012.03.038.

Chen, P., Pei, D.C.T., 1984. Fluidization characteristics of fine particles. Can. J. Chem. Eng. 62 (4), 464–468. https://doi.org/10.1002/cjce.5450620403.

Dekkers, S., Bouwmeester, H., Bos, P.M., Peters, R.J., Rietveld, A.G., Oomen, A.G., 2013. Knowledge gaps in risk assessment of nanosilica in food: evaluation of the dissolution and toxicity of different forms of silica. Nanotoxicology 7 (4), 367–377. https://doi.org/10.3109/17435390.2012.662250.

Feng, L., Liu, Z., 2011. Graphene in biomedicine: opportunities and challenges. Nanomedicine (London, England) 6, 317–324. https://doi.org/10.2217/nnm.10.158.

Han, W., Mai, B., Gu, T., 1991. Residence time distribution and drying characteristics of a continous vibro-fluidized bed. Dry. Technol. 9 (1), 159–181. https://doi.org/10.1080/07373939108916645.

He, Z., Zhang, Z., Bi, S., 2020. Nanoparticles for organic electronics applications. Mater. Res. Express 7. https://doi.org/10.1088/2053-1591/ab636f.

Iwadate, Y., Horio, M., 1998. Prediction of agglomerate sizes in bubbling fluidized beds of group C powders. Powder Technol. 100 (2), 223–236. https://doi.org/10.1016/S0032-5910(98)00143-0.

Jaraiz, E., Kimura, S., Levenspiel, O., 1992. Vibrating beds of fine particles: estimation of interparticle forces from expansion and pressure drop experiments. Powder Technol. 72 (1), 23–30. https://doi.org/10.1016/S0032-5910(92)85017-P.

Jiang, Z., Fatah, N., 2022. New investigation of micro-fluidized bed: the effect of wall roughness and particle size on hydrodynamics regimes. Chem. Eng. J. 430, 133075. https://doi.org/10.1016/j.cej.2021.133075.

Kaliyaperumal, S., Barghi, S., Briens, L., Rohani, S., Zhu, J., 2011. Fluidization of nano and sub-micron powders using mechanical vibration. Particuology 9 (3), 279–287. https://doi.org/10.1016/j.partic.2011.03.003.

Kamphorst, R., Wu, K., Salameh, S., Meesters, G.M.H., van Ommen, J.R., 2022. On the fluidization of cohesive powders: differences and similarities between micro- and nano-sized particle gas–solid fluidization. Can. J. Chem. Eng. https://doi.org/10.1002/cjce.24615.

Kamphorst, R., van der Sande, P.C., Wu, K., Wagner, E.C., David, M.K., Meesters, G.M., van Ommen, J.R., 2023. The mechanism behind vibration assisted fluidization of cohesive micro-silica. KONA Powder Part. J., 2024007. https://doi.org/10.14356/kona.2024007.

Kamphorst, R., Wanjari, P., Saedy, S., van Dam, J.F., Thijssen, A., Brüner, P., Grehl, T., Meesters, G.M., van Ommen, J.R., 2024. Enhancing colloid stability of polymer microspheres in water through SiO_2 coating: effects of coating cycles and surface coverage. Surf. Interfaces 45, 103852. https://doi.org/10.1016/j.surfin.2024.103852.

Lee, J.-R., Hasolli, N., Lee, K.-S., Lee, K.-Y., Park, Y.O., 2019. Fluidization of fine powder assisted by vertical vibration in fluidized bed reactor. Korean J. Chem. Eng. 36, 1548–1556. https://doi.org/10.1007/s11814-019-0339-2.

Li, J., Liang, X., King, D.M., Jiang, Y.-B., Weimer, A.W., 2010. Highly dispersed Pt nanoparticle catalyst prepared by atomic layer deposition. Appl. Catal. B, Environ. 97 (1), 220–226. https://doi.org/10.1016/j.apcatb.2010.04.003.

Marring, E., Hoffmann, A., Janssen, L., 1994. The effect of vibration on the fluidization behaviour of some cohesive powders. Powder Technol. 79 (1), 1–10. https://doi.org/10.1016/0032-5910(94)02810-9.

Matsui, I., 2005. Nanoparticles for electronic device applications: a brief review. J. Chem. Eng. Jpn. 38, 535–546. https://doi.org/10.1252/jcej.38.535.

Mawatari, Y., Koide, T., Ikegami, T., Tatemoto, Y., Noda, K., 2003. Characteristics of vibro-fluidization for fine powder under reduced pressure. Adv. Powder Technol. 14 (5), 559–570. https://doi.org/10.1163/156855203322448345.

Mawatari, Y., Hamada, Y., Yamamura, M., Kage, H., 2015. Flow pattern transition of fine cohesive powders in a gassolid fluidized bed under mechanical vibrating conditions. Proc. Eng. 102, 945–951. https://doi.org/10.1016/j.proeng.2015.01.216. New Paradigm of Particle Science and Technology Proceedings of the 7th World Congress on Particle Technology.

Mogre, C., Thakurdesai, A.U., van Ommen, J.R., Salameh, S., 2017. Long-term fluidization of titania nanoparticle agglomerates. Powder Technol. 316, 441–445. https://doi.org/10.1016/j.powtec.2017.01.074. Fluidization for Emerging Green Technologies.

Mohseni, M., Kolomijtschuk, A., Peters, B., Demoulling, M., 2019. Biomass drying in a vibrating fluidized bed dryer with a Lagrangian-Eulerian approach. Int. J. Therm. Sci. 138, 219–234. https://doi.org/10.1016/j.ijthermalsci.2018.12.038.

Morooka, S., Kusakabe, K., Kobata, A., Kato, Y., 1988. Fluidization state of ultrafine powders. J. Chem. Eng. Jpn. 21 (1), 41–46. https://doi.org/10.1252/jcej.21.41.

Nam, C., Pfeffer, R., Dave, R., Sundaresan, S., 2004. Aerated vibrofluidization of silica nanoparticles. AIChE J. 50, 1776–1785. https://doi.org/10.1002/aic.10237.

Pacek, A., Nienow, A., 1990. Fluidisation of fine and very dense hardmetal powders. Powder Technol. 60 (2), 145–158. https://doi.org/10.1016/0032-5910(90)80139-P.

Qu, L., Liu, Y., Baek, J.-B., Dai, L., 2010. Nitrogen-doped graphene as efficient metal-free electrocatalyst for oxygen reduction in fuel cells. ACS Nano 4, 1321–1326. https://doi.org/10.1021/nn901850u.

Raganati, F., Chirone, R., Ammendola, P., 2018. Gas–solid fluidization of cohesive powders. Chem. Eng. Res. Des. 133, 347–387. https://doi.org/10.1016/j.cherd.2018.03.034.

Satija, S., Zucker, I., 1986. Hydrodynamics of vibro-fluidized beds. Dry. Technol. 4 (1), 19–43. https://doi.org/10.1080/07373938608916309.

Seville, J., Willett, C., Knight, P., 2000. Interparticle forces in fluidisation: a review. Powder Technol. 113 (3), 261–268. https://doi.org/10.1016/S0032-5910(00)00309-0. Neptis Symposium on Fluidization – Present and Future.

Shen, D., Gu, S., 2009. The mechanism for thermal decomposition of cellulose and its main products. Bioresour. Technol. 100 (24), 6496–6504. https://doi.org/10.1016/j.biortech.2009.06.095.

Valverde, J.M., Castellanos, A., 2006. Effect of compaction history on the fluidization behavior of fine cohesive powders. Phys. Rev. E 73, 056310. https://doi.org/10.1103/PhysRevE.73.056310.

Van Ommen, J.R., Valverde, J.M., Pfeffer, R., 2012. Fluidization of nanopowders: a review. J. Nanopart. Res. 14. https://doi.org/10.1007/s11051-012-0737-4.

Wang, Y., Yuan, L., Yao, C., Ding, L., Li, C., Fang, J., Sui, K., Liu, Y., Wu, M., 2014. A combined toxicity study of zinc oxide nanoparticles and vitamin C in food additives. Nanoscale 6, 15333–15342. https://doi.org/10.1039/C4NR05480F.

Wang, Z., Kwauk, M., Li, H., 1998. Fluidization of fine particles. Chem. Eng. Sci. 53 (3), 377–395. https://doi.org/10.1016/S0009-2509(97)00280-7.

Wu, K., Wagner, E., Ochkin-Koenig, O., Franck, M., Weis, D., Meesters, G., Van Ommen, J.R., 2023. Time-resolved x-ray study of assisted fluidization of cohesive micron powder: on the role of mechanical vibration. Chem. Eng. J. 470, 143936. https://doi.org/10.1016/j.cej.2023.143936.

Yang, J., Zhou, T., Song, L., 2009. Agglomerating vibro-fluidization behavior of nanoparticles. Adv. Powder Technol. 20 (2), 158–163. https://doi.org/10.1016/j.apt.2008.06.002.

Yao, W., Guangsheng, G., Fei, W., Jun, W., 2002. Fluidization and agglomerate structure of SiO_2 nanoparticles. Powder Technol. 124 (1), 152–159. https://doi.org/10.1016/S0032-5910(01)00491-0.

Zeng, P., Zhou, T., Yang, J., 2008. Behavior of mixtures of nano-particles in magnetically assisted fluidized bed. Chem. Eng. Process., Process Intensif. 47 (1), 101–108. https://doi.org/10.1016/j.cep.2007.08.009.

Zhang, W., Zhao, M., 2010. Fluidisation behaviour of silica nanoparticles under horizontal vibration. J. Exp. Nanosci. 5 (1), 69–82. https://doi.org/10.1080/17458080903260944.

Zhou, E., Zhang, Y., Zhao, Y., Luo, Z., He, J., Duan, C., 2018. Characteristic gas velocity and fluidization quality evaluation of vibrated dense medium fluidized bed for fine coal separation. Adv. Powder Technol. 29 (4), 985–995. https://doi.org/10.1016/j.apt.2018.01.017.

Zhu, C., Yu, Q., Dave, R., Pfeffer, R., 2005. Gas fluidization characteristics of nanoparticle agglomerates. AIChE J. 51, 426–439. https://doi.org/10.1002/aic.10319.